

Supporting Information for

**Near-infrared Electron Acceptors with Fused Nonacyclic Molecular Backbones  
for Nonfullerene Organic Solar Cells**

Jianquan Zhang,<sup>‡ab</sup> Yunke Li,<sup>‡b</sup> Zhengxing Peng,<sup>‡d</sup> Fujin Bai,<sup>b</sup> Lik-Kuen Ma,<sup>b</sup> Harald Ade,<sup>\*d</sup> Zhengke Li,<sup>\*a</sup> He Yan<sup>\*bc</sup>

<sup>a</sup> Key Laboratory for Polymeric Composite and Functional Materials of Ministry of Education, School of Materials and Engineering, Sun Yet-Sen University, Guangzhou 510275, China

<sup>b</sup> Department of Chemistry, Hong Kong University of Science and Technology (HKUST), Clear Water Bay, Kowloon, Hong Kong SAR, P. R. China

<sup>c</sup> Hong Kong University of Science and Technology-Shenzhen Research Institute, No. 9, Yuexing 1st RD, Hi-tech Park, Nanshan, Shenzhen 518057, P. R. China

<sup>d</sup> Department of Physics and Organic and Carbon Electronics Laboratory, North Carolina State University, Raleigh, North Carolina 27695, United States

<sup>‡</sup> These authors contributed equally to this work.

**General Information.**

$^1\text{H}$  and  $^{13}\text{C}$  NMR spectra were recorded on a Bruker AV-400 MHz NMR spectrometer. Chemical shifts are reported in parts per million (ppm,  $\delta$ ).  $^1\text{H}$  NMR and  $^{13}\text{C}$  NMR spectra were referenced to tetramethylsilane (0 ppm) for  $\text{CDCl}_3$ . Mass spectra were collected on a MALDI Micro MX mass spectrometer, or an API QSTAR XL System.

**Materials.** IDTT-4Cl was purchased from Solarmer and PTB7-Th was purchased from 1-Material. Tetrahydrofuran was freshly distilled before use from sodium using benzophenone as the indicator. All other reagents and chemicals were purchased from commercial sources and used without further purification.

**Optical characterizations.** Film UV-Vis absorption spectra were acquired on a Perkin Elmer Lambda 20 UV/VIS Spectrophotometer. The films were cast from the solutions of the acceptors with a concentration of 20 mg/mL in chloroform. UV-Vis absorption spectra were collected from the solution of two small molecules with the concentration of  $1.0 \times 10^{-6}$  M in chloroform and a cuvette with a stopper (Sigma Z600628) was used to avoid volatilization during the measurement.

**Electrochemical characterizations.** Cyclic voltammetry was carried out on a CHI610E electrochemical workstation with three electrodes configuration, using Ag/AgCl as the reference electrode, a Pt plate as the counter electrode, and a glassy carbon as the working electrode.  $0.1 \text{ mol L}^{-1}$  tetrabutylammonium hexafluorophosphate in anhydrous acetonitrile was used as the supporting electrolyte. The solid films were drop-casted on the working electrode from a chloroform solution with a concentration of 5 mg/mL. Potentials were referenced to the ferrocenium/ferrocene couple by using ferrocene as external standards in acetonitrile solutions. The scan rate is  $0.05 \text{ V s}^{-1}$ . The LUMO levels were estimated by  $-(E_{\text{re}} - E_{\text{fc}} + 4.8) \text{ eV}$  and the HOMO levels were estimated by  $-(E_{\text{ox}} - E_{\text{fc}} + 4.8) \text{ eV}$ .

**AFM analysis.** AFM measurements were performed by using a Scanning Probe Microscope Dimension 3100 in tapping mode. All film samples were spin-cast on ITO/ZnO substrates.

**Solar cell fabrication and testing.** Diethylzinc (15 % wt in toluene) and molybdenum oxide ( $\text{MoO}_3$ ) were purchased from Sigma-Aldrich and used as received without further treatment. Pre-patterned ITO-coated glass substrates were cleaned by sequential sonication in soap deionized water, deionized water, acetone, and isopropanol for 30 min of each step. Active layer solutions (D:A ratio 1:1.5 w/w) were

prepared in chloroform with 0.5% 1,8-diiodooctane (polymer concentration: 8 mg mL<sup>-1</sup>). To completely dissolve the polymer, the active layer solution should be stirred on a hotplate at 65 °C for at least 1 hour. The active layers were spin-coated with a speed of 2000-300 rpm at room temperature. The active layers were then treated with vacuum to remove the solvent. Subsequently, the blend films were thermally annealed at 100 °C for 5 min before being transferred to the vacuum chamber of a thermal evaporator inside the same glovebox, and a thin layer (6 nm) of MoO<sub>3</sub> was deposited as the anode interlayer, followed by the deposition of 100 nm of Al as the top electrode at a vacuum level of  $\sim 1.0 \times 10^{-4}$  Pa. All devices were encapsulated using epoxy and thin glass slides inside the glovebox. Device *J-V* characteristics were measured under AM 1.5G (100 mW cm<sup>-2</sup>) using a Newport solar simulator in ambient atmosphere. The light intensity was calibrated using a standard Si diode (with KG5 filter, purchased from PV Measurement) to bring spectral mismatch to unity. *J-V* characteristics were recorded using a Keithley 2400 source meter unit. Typical cells have devices area of 5.9 mm<sup>2</sup>, defined by a metal mask with an aperture aligned with the device area.

**EQE measurements.** EQEs were measured using an Enlitech QE-S EQE system equipped with a standard Si diode. Monochromatic light was generated from a Newport 300W lamp source.

**Mobility measurements.** The mobilities were measured using the space charge limited current (SCLC) method, employing a device architecture of ITO/ZnO/blend film/MoO<sub>3</sub>/Al for hole-only devices and ITO/ZnO/blend film/Ca/Al for electron-only devices. The mobilities were obtained by taking current-voltage curves and fitting the results to a space charge limited form, where the SCLC is described by:

$$J = \frac{9\varepsilon_0\varepsilon_r\mu(V_{\text{appl}} - V_{\text{bi}} - V_s)^2}{8L^3}$$

Where  $\varepsilon_0$  is the permittivity of free space,  $\varepsilon_r$  is the relative permittivity of the material (assumed to be 3),  $\mu$  is the hole mobility and  $L$  is the thickness of the film. From the plots of  $J^{1/2}$  vs  $V_{\text{appl}} - V_{\text{bi}} - V_s$ , hole or electron mobilities can be deduced.

**GIWAXS characterization.** GIWAXS measurements were performed at beamline 7.3.3 at the Advanced Light Source. Samples were prepared on Si substrates using identical blend solutions like those used in devices. The 10 keV X-ray beam was incident at a grazing angle of 0.11° - 0.15°, which maximized the scattering intensity from the samples. The scattered X-rays were detected using a Dectris Pilatus 2M photon

counting detector. In-plane and out-of-plane sector averages were calculated using the Nika software package. The coherence length was calculated using the Scherrer equation:

$$L_c = \frac{2\pi K}{\Delta q}$$

**R-SoXS characterization.** R-SoXS transmission measurements were performed at beamline 11.0.1.2 at the Advanced Light Source. Samples for R-SoXS measurement were prepared on a PSS modified Si substrate under the same conditions as those used for device fabrication, and then transferred by floating in water to a 1.5 mm × 1.5 mm, 100 nm thick Si<sub>3</sub>N<sub>4</sub> membrane supported by a 5 mm × 5 mm, 200 μm thick Si frame (Norcada Inc.). 2D scattering patterns were collected on an in-vacuum CCD camera (Princeton Instrument PI-MTE). The sample detector distance was calibrated from diffraction peaks of a triblock copolymer poly(isoprene-b-styrene-b-2-vinyl pyridine), which has a known spacing of 391 Å. The beam size at the sample is approximately 100 μm by 200 μm.

**Contact Angle Measurements.** Contact angles were measured with a contact angle meter (GBX DIGIDROP). The solution of each pure organic material was spin-coated on cleaned ITO substrates. Droplets of two different liquids, water and ethylene glycol (EG) were cast onto the pure organic films with the drop size kept at 4 μL per drop. Contact angle images were taken at 1 s after the whole droplet was deposited onto the sample surface. At least 3 independent measurements were performed for each single liquid. The surface tension of each pure material was calculated by

$$\gamma_{water}(1 + \cos\theta_{water}) = 2 \sqrt{\gamma_{water}^d \gamma^d} + 2 \sqrt{\gamma_{water}^p \gamma^p}$$

$$\gamma_{EG}(1 + \cos\theta_{EG}) = 2 \sqrt{\gamma_{EG}^d \gamma^d} + 2 \sqrt{\gamma_{EG}^p \gamma^p}$$

$$\gamma_{total} = \gamma^d + \gamma^p$$

where  $\theta$  is the droplet contact angle on the organic thin film;  $\gamma_{total}$  is the surface tension of the organic material, which is equal to the sum of the dispersion ( $\gamma^d$ ) and polarity ( $\gamma^p$ ) components;  $\gamma_i$  is the surface tension of the liquid droplet (water or EG);  $\gamma^d$  and  $\gamma^p$  are the dispersion and polarity components of  $\gamma_{total}$ , respectively.<sup>1</sup>

For non-polar materials a linear relationship exists between the solubility parameter ( $\delta$ ) and the square root of  $\gamma_{total}$ , where  $K$  is a universal proportionality constant ( $K = 116 \times 10^3 \text{ m}^{-1/2}$ ):

$$\delta = K\sqrt{\gamma_{total}}$$

The dimensionless Flory–Huggins parameter representing the enthalpic interaction between components  $i$  and  $j$  is calculated by:

$$\chi_{ij} = \frac{V_0}{RT}(\delta_i - \delta_j)^2 + \chi_s$$

where  $\chi_s$  is the entropic contribution to the interaction parameter with an often used value of 0.34, for a nonpolar polymer in a non-polar solvent.  $V_0$  is the molar volume of the polymer, which is generated by theoretical calculations ( $V_{0, \text{PTB7-Th}} = 737 \text{ cm}^3/\text{mol}$ ). Noted that the precise value adopted is not critical.

**Table S1.** Average values of contact angle, surface tension and solubility parameters of individual materials calculated from three independent measurements.

<b>Materials</b>	$\theta_{\text{water}}$ [°]	$\theta_{\text{EG}}$ [°]	$\gamma_{\text{d}}$ [mN/m]	$\gamma_{\text{p}}$ [mN/m]	$\gamma_{\text{total}}$ [mN/m]	$\delta$ [MPa <sup>1/2</sup> ]
PTB7-Th	98.3	73.4	21.8	1.7	23.5	17.8
IDTT-4Cl	94.1	73.9	15.6	4.6	20.2	16.5
CPDT-4Cl	93.9	66.9	25.3	2.1	27.4	19.2
DTPR-4Cl	94.2	66.8	25.7	2.0	27.7	19.3

**Table S2.** Device performances of the three blends with an inverted device structure with or without 0.5% DIO as the additive.

	<b>Additive</b>	$V_{OC}$	$J_{SC}$	<b>FF</b>	<b>Highest PCE</b>
		(V)	(mA cm <sup>-2</sup> )	(%)	(%)
PTB7-Th:	/	0.61±0.01	16.45±0.32	61.2±0.2	6.33
IDTT-4Cl	0.5% DIO	0.61±0.01	18.34±0.46	64.3±0.1	7.70
PTB7-Th:	/	0.75±0.01	21.64±0.27	66.1±0.2	11.12
CPDT-4Cl	0.5% DIO	0.74±0.01	23.24±0.47	69.1±0.2	12.15
PTB7-Th:	/	0.67±0.01	23.88±0.20	60.1±0.1	9.95
DTPR-4Cl	0.5% DIO	0.68±0.01	24.97±0.21	61.8±0.1	10.75

**Table S3.** SCLC mobilities of the pristine and blend films.

<b>Material combinations</b>	$\mu_h$	$\mu_e$
	(cm <sup>2</sup> V <sup>-1</sup> s <sup>-1</sup> )	(cm <sup>2</sup> V <sup>-1</sup> s <sup>-1</sup> )
IDTT-4Cl	/	(2.50±0.25)×10 <sup>-4</sup>
CPDT-4Cl	/	(3.64±0.19)×10 <sup>-4</sup>
DTPR-4Cl	/	(2.12±0.21)×10 <sup>-4</sup>
PTB7-Th:IDTT-4Cl	(1.64±0.23)×10 <sup>-4</sup>	(2.10±0.27)×10 <sup>-4</sup>
PTB7-Th:CPDT-4Cl	(1.90±0.17)×10 <sup>-4</sup>	(3.07±0.15)×10 <sup>-4</sup>
PTB7-Th:DTPR-4Cl	(1.73±0.22)×10 <sup>-4</sup>	(1.42±0.31)×10 <sup>-4</sup>

**Table S4.** Summary of device performances based on PTB7-Th:IDTT-type low-bandgap acceptors.

<b>Donor</b>	<b>Acceptor</b>	$E_g$ (eV)	$V_{oc}$ (V)	$J_{sc}$ (mA cm <sup>-2</sup> )	<b>FF</b> (%)	<b>PCE</b> (%)	<b>Ref</b>
PTB7-Th	CO <sub>8</sub> DFIC	1.26	0.68	26.1	68	12.2	<i>Sci. Bull.</i> , 2017, 62, 1494
PTB7-Th	BT-CIC	1.33	0.70	22.5	71	11.6	<i>JACS</i> 2017, 139, 17114
PTB7-Th	DTPC-DFIC	1.21	0.76	21.9	61	10.2	<i>JACS</i> 2018, 140, 2054
PTB7-Th	IEICO-4Cl	1.24	0.73	22.8	62	10.3	<i>Adv. Mater.</i> 2017, 1703080
PTB7-Th	FOIC	1.32	0.74	23.5	67	12.0	<i>Adv. Mater.</i> 2018, 30, 1705969
PTB7-Th	T2	1.30	0.65	24.9	67	10.9	<i>Adv. Mater.</i> 2018, 30, 1803769
PTB7-Th	F8IC	1.27	0.64	25.1	68	10.9	<i>Adv. Mater.</i> 2018, 30, 1706571
PTB7-Th	IUIC	1.41	0.79	21.5	64	11.2	<i>Chem. Mater.</i> , 2018, 30, 239
PTB7-Th	4TO-T-4F	1.30	0.75	20.4	58	8.9	<i>Mater. Chem. Front.</i> , 2019, 3,
PTB7-Th	4TO-Se-4F	1.27	0.70	19.1	56	7.4	2157
PTB7-Th	SiOTIC-4F	1.17	0.65	21.6	62	9.0	<i>Adv. Energy Mater.</i> 2018, 8,
PTB7-Th	COTIC-4F	1.10	0.56	20.3	56	7.4	1801212
PTB7-Th	CPDT-4Cl	1.35	0.74	23.2	69	12.2	<i>This work</i>
PTB7-Th	DTPR-4Cl	1.30	0.68	25.0	62	10.8	<i>This work</i>

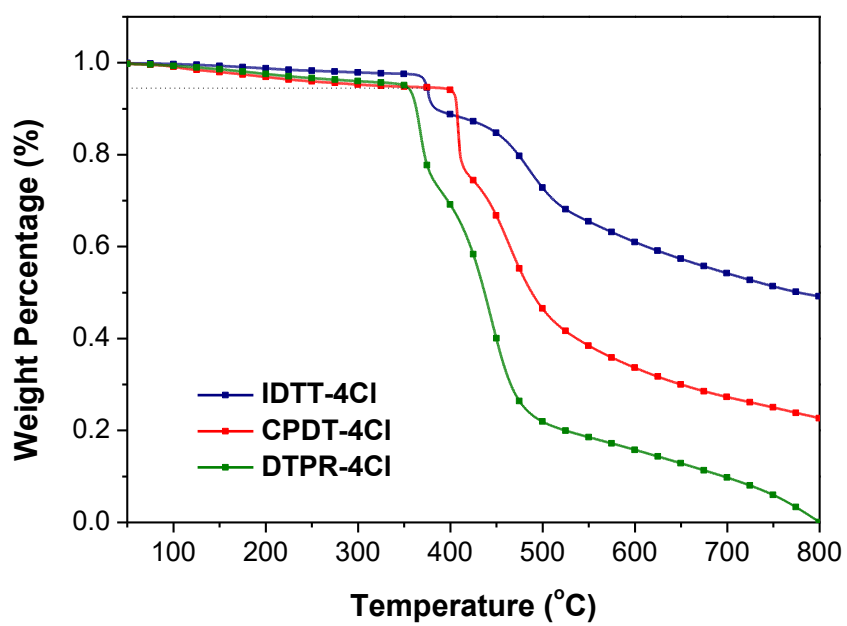
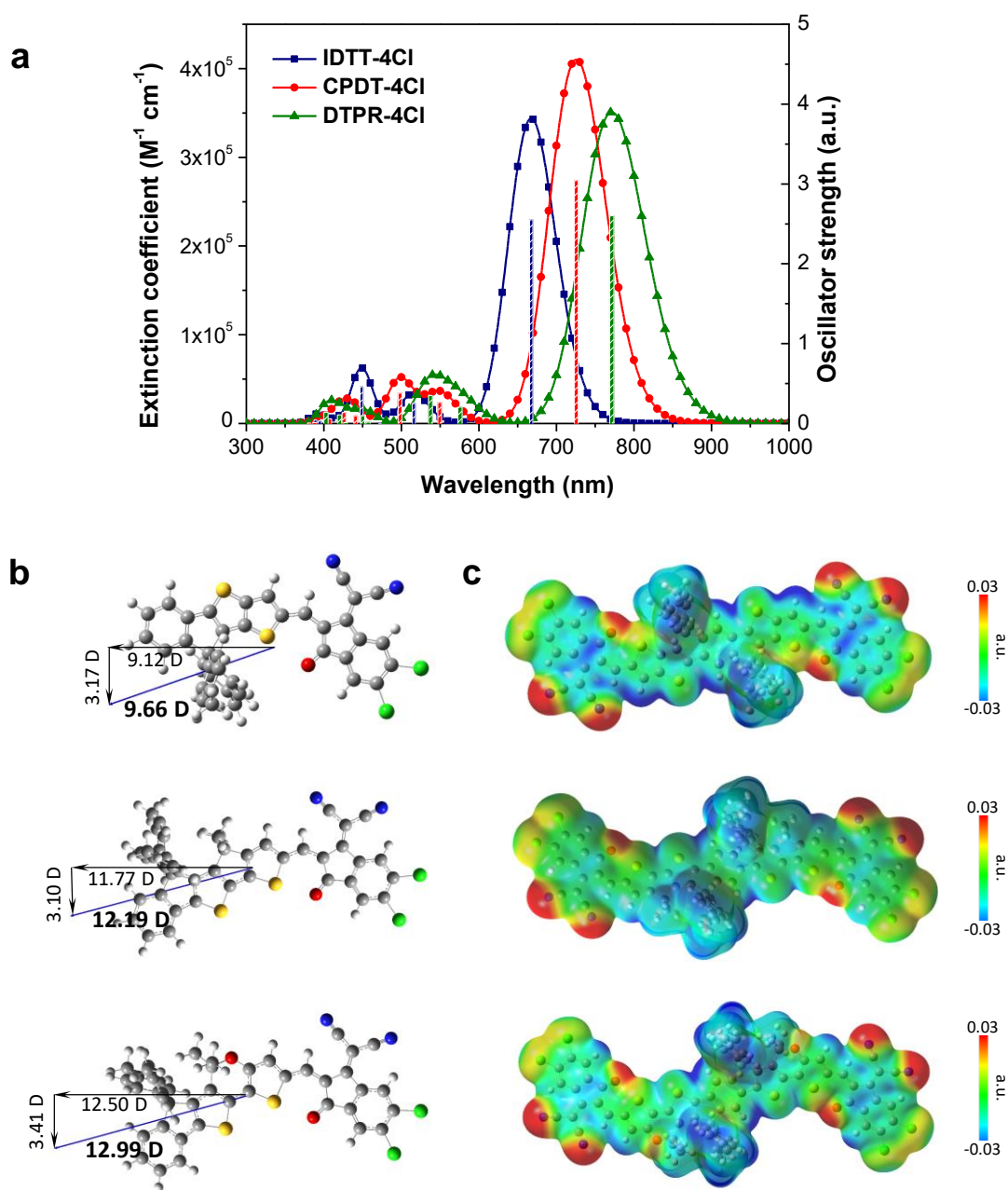
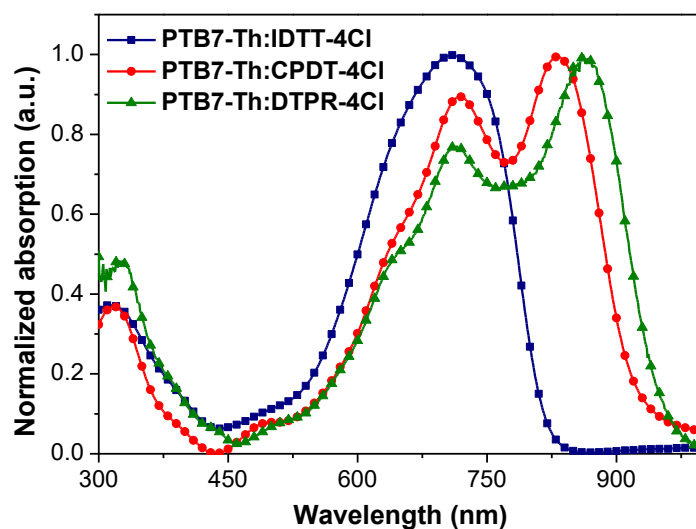


Figure S1. TGA curves of IDTT-4Cl, CPDT-4Cl and DTPR-4Cl.



**Figure S2.** (a) Computed UV-Vis absorption; (b) dipole moment; and (c) electrostatic potential graphs of IDTT-4Cl, CPDT-4Cl and DTPR-4Cl.



**Figure S3.** UV-Vis absorption of the PTB7-Th:IDTT-4Cl, PTB7-Th:CPDT-4Cl and PTB7-Th:DTPR-4Cl blend films.

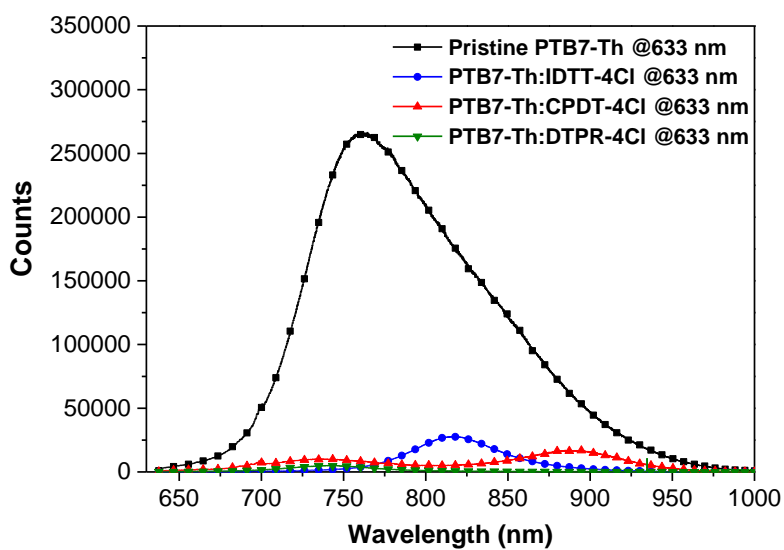


**Figure S4.** Photoluminescence quenching experiments of the PTB7-Th:IDTT-4Cl, PTB7-Th:CPDT-4Cl and PTB7-Th:DTPR-4Cl blend films with the excitation wavelength of 633 nm.

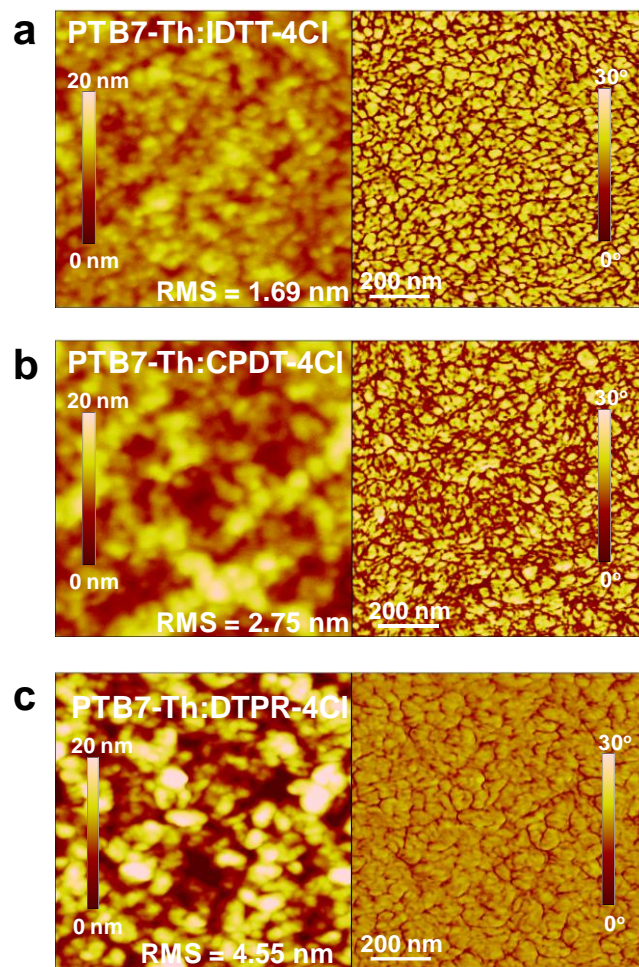


**Figure S5.** AFM images ( $1\ \mu\text{m}\times 1\ \mu\text{m}$ , left: height images and right: phase images) of the (a) PTB7-Th:IDTT-4Cl, (b) PTB7-Th:CPDT-4Cl and (c) PTB7-Th:DTPR-4Cl blend films.

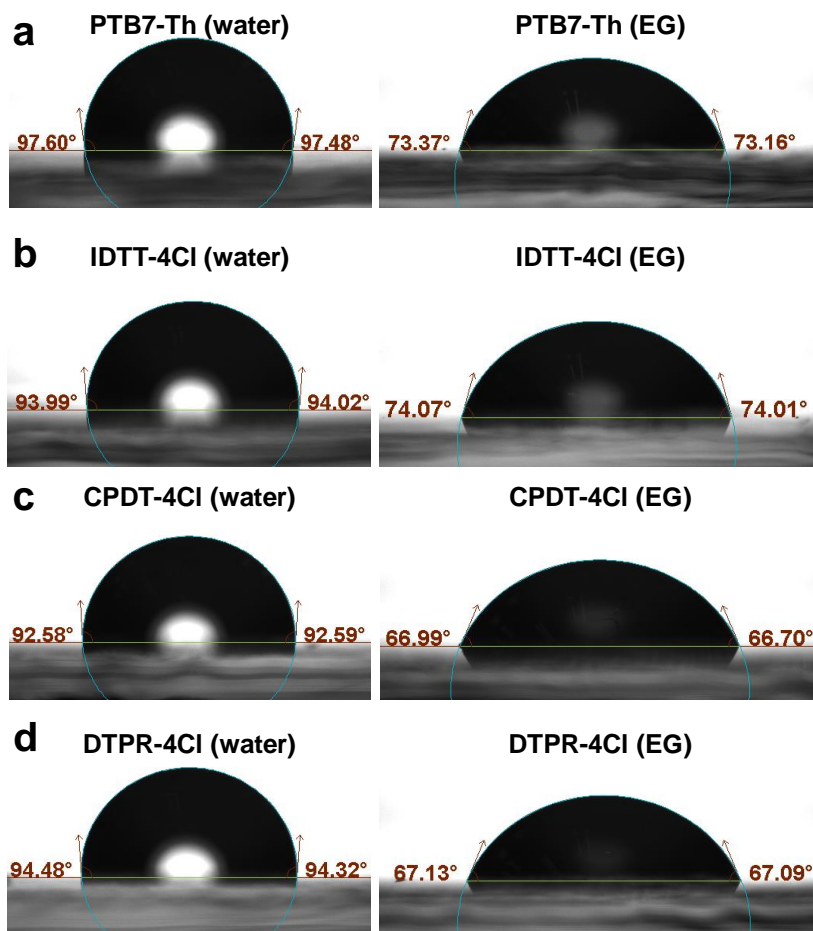


**Figure S6.** Contact angle measurements of the thin film of (d) PTB7-Th, (e) IDTT-4Cl, (f) CPDT-4Cl and (g) DTPR-4Cl.

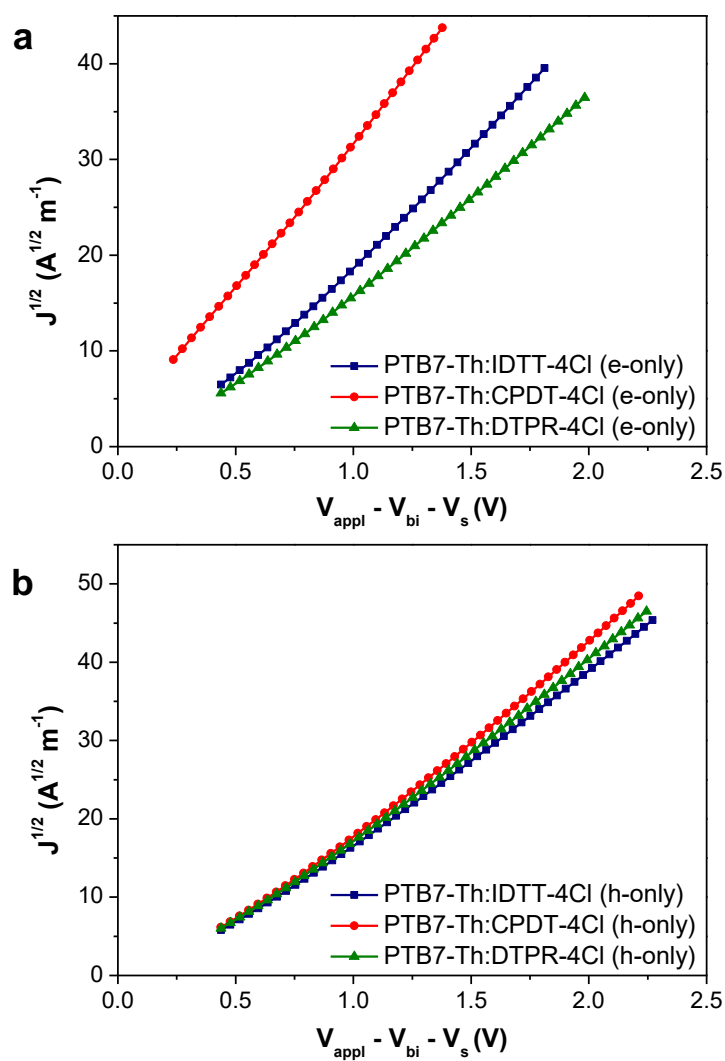


**Figure S7.** Mobility measurement of (a) electron-only and (b) hole-only devices of the PTB7-Th:IDTT-4Cl, PTB7-Th:CPDT-4Cl and PTB7-Th:DTPR-4Cl blend films.

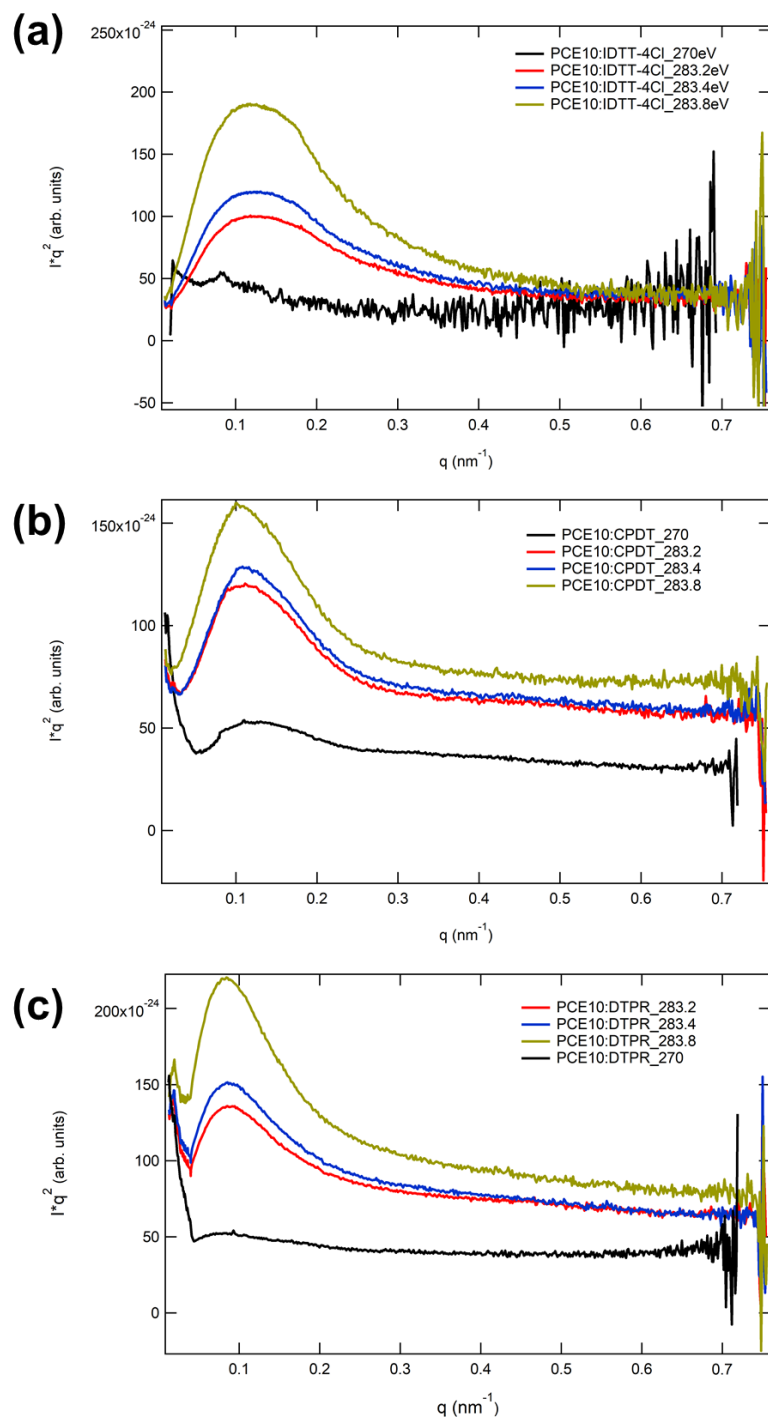
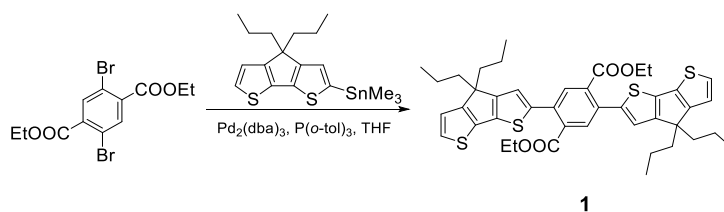


**Figure S8.** Lorentz corrected RSoXS profile at different beam energies of the (a) PTB7-Th:IDTT-4Cl, (b) PTB7-Th:CPDT-4Cl and (c) PTB7-Th:DTPR-4Cl blend films.

## Synthesis.

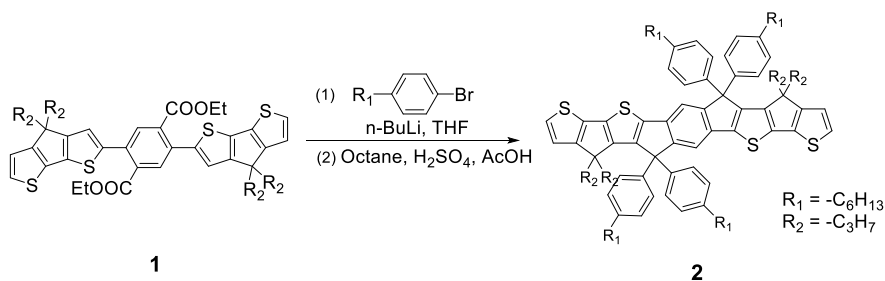


**Synthesis of compound 1.** To a mixture of diethyl 2,5-dibromoterephthalate (500 mg, 1.32 mmol), (4,4-dipropyl-4H-cyclopenta[2,1-b:3,4-b']dithiophen-2-yl)trimethylstannane (1.34 g, 3.16 mmol), Pd<sub>2</sub>(dba)<sub>3</sub> (121 mg, 0.13 mmol) and P(*o*-tol)<sub>3</sub> (320 mg, 1.05 mmol) was added anhydrous THF (10 mL) under N<sub>2</sub>. The reaction mixture was stirred for 12 h at 80 °C. Then, the reaction mixture was cooled and poured into an aqueous potassium fluoride. The mixture was extracted with diethyl ether for three times. The combined organic phase was washed with water followed by brine. Then the solution was dried over Na<sub>2</sub>SO<sub>4</sub> and concentrated under reduced pressure. The residue was purified by column chromatography (stationary phase: silica gel; eluent: n-hexane:dichloromethane = 2:1) to get the product as yellow solid (743 mg, 76%).

<sup>1</sup>H NMR (400 MHz, CDCl<sub>3</sub>) δ 7.82 (s, 2H), 7.23 (d, *J* = 4.9 Hz, 2H), 6.99 (s, 2H), 6.98 (d, *J* = 4.9 Hz, 2H), 4.26 (q, 4H), 1.86 (t, 8H), 1.21 (t, *J* = 7.1 Hz, 6H), 1.03 (dt, 8H), 0.80 (t, 12H).

<sup>13</sup>C NMR (100 MHz, CDCl<sub>3</sub>) δ 168.6, 158.4, 158.1, 139.9, 137.9, 136.3, 133.7, 132.9, 131.1, 125.4, 121.6, 77.4, 77.1, 76.7, 61.8, 53.9, 40.2, 18.0, 14.4, 13.9.

MALDI-TOF MS: Calcd for C<sub>42</sub>H<sub>46</sub>O<sub>4</sub>S<sub>4</sub> (M<sup>+</sup>): 742.2279, Found: 742.2282.



**Synthesis of compound 2.** *n*-BuLi (5.1 mL, 2.0 M in hexane) was added dropwise to a solution of 1-bromo-4-hexylbenzene (2.60 g, 10.78 mmol) in anhydrous THF (50 mL) at -78 °C under N<sub>2</sub> atmosphere. The stirred mixture was kept at the same temperature

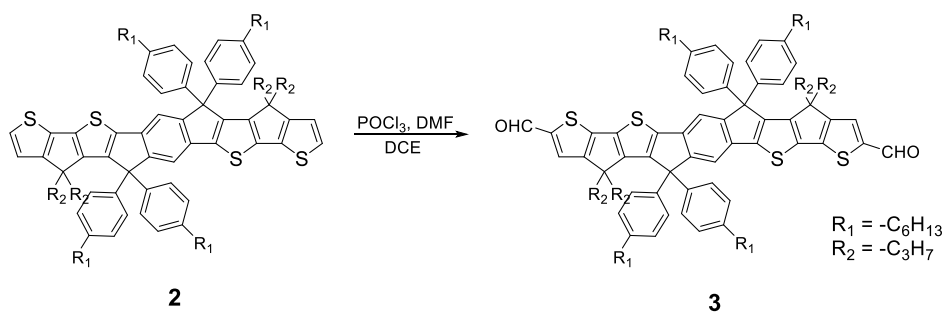
for 1 h and then added into a degassed solution of compound 1 (500 mg, 0.673 mmol) in THF (10 mL) via syringe. When the addition was completed, the resulting mixture was stirred -78 °C for 2 h, followed by quenching with a saturated NH<sub>4</sub>Cl solution. The organic layer was separated, and the aqueous phase was extracted with diethyl ether for three times. The combined organic layer was washed with brine, dried over MgSO<sub>4</sub>, filtered, and concentrated under reduced pressure to obtain a crude diol as a viscous oil, which could be directly used for the next step without further purification.

The crude diol obtained above was dissolved in a mixture of octane (10 mL) and acetic acid (10 mL) and then three drops of concentrated H<sub>2</sub>SO<sub>4</sub> was added. After being stirred for 1 h at r.t., water was added into the mixture to quench the reaction. The organic layer was separated, and the aqueous phase was extracted with diethyl ether for three times. The combined organic layer was washed with brine, dried over MgSO<sub>4</sub>, filtered, and concentrated under reduced pressure. The residue was purified by column chromatography (stationary phase: silica gel; eluent: n-hexane:dichloromethane = 20:1) to get the product as yellow solid (519 mg, 61%, 2 steps).

<sup>1</sup>H NMR (400 MHz, CDCl<sub>3</sub>) δ 7.33 (d, 8H, *J* = 8.0 Hz), 7.15 (s, 2H), 7.09 (d, 8H, *J* = 8.0 Hz), 7.08 (d, 2H, *J* = 4.4 Hz), 6.78 (d, 2H, 4.4 Hz), 2.60 (t, 8H), 1.61 (t, 8H), 1.50-1.27 (m, 32H), 0.95-0.83 (t, 12H), 0.59-0.41 (m, 8H), 0.41-0.28 (t, 12H).

<sup>13</sup>C NMR (100 MHz, CDCl<sub>3</sub>) δ 157.3, 156.3, 151.9, 151.3, 142.6, 141.5, 139.8, 139.5, 136.6, 134.8, 128.8, 128.1, 124.2, 121.5, 114.6, 63.2, 55.2, 39.7, 35.6, 31.8, 31.4, 29.7, 29.2, 22.6, 17.3, 14.1, 13.9.

MALDI-TOF MS: Calcd for C<sub>86</sub>H<sub>102</sub>S<sub>4</sub> (M<sup>+</sup>): 1262.6864, Found: 1262.6869.

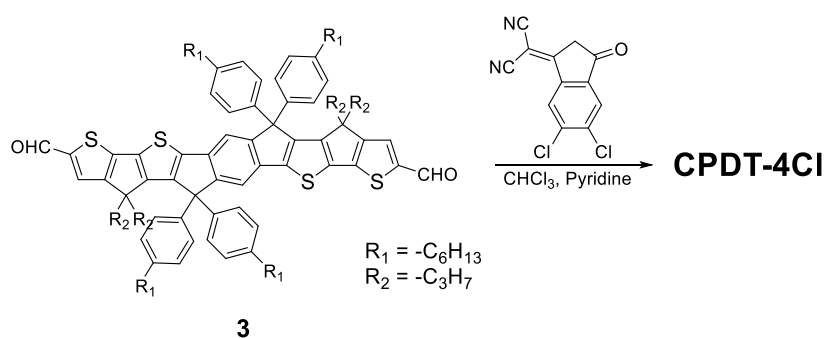


**Synthesis of compound 3.** Compound 2 (200 mg, 0.158 mmol) was dissolved in 20 mL dichloroethane under argon, then the fresh Vilsmeier reagent (0.2 mL POCl<sub>3</sub> in 1.0 mL DMF) was added dropwise at 0 °C. The mixture was stirred at 85 °C for 3 h. The reaction was quenched with saturated Na<sub>2</sub>CO<sub>3</sub> solution and allowed to stir at r.t. for 20 mins. The organic layer was separated, and the aqueous phase was extracted with diethyl ether for three times. The combined organic layer was washed with brine, dried over MgSO<sub>4</sub>, filtered, and concentrated under reduced pressure. The residue was purified by column chromatography (stationary phase: silica gel; eluent: dichloromethane) to get the product as orange-red solid (176 mg, 88%).

<sup>1</sup>H NMR (400 MHz, CDCl<sub>3</sub>) δ 9.79 (s, 2H), 7.41 (s, 2H), 7.31 (d, 8H, *J* = 8.0 Hz), 7.23 (s, 2H), 7.11 (d, 8H, *J* = 8.0 Hz), 2.60 (t, 8H), 1.62 (t, 8H), 1.50-1.25 (m, 32H), 0.96-0.85 (t, 12H), 0.64-0.35 (m, 8H), 0.35-0.25 (t, 12H).

<sup>13</sup>C NMR (100 MHz, CDCl<sub>3</sub>) δ 182.3, 157.3, 157.2, 156.3, 151.6, 147.8, 147.5, 142.7, 142.0, 139.0, 138.8, 135.2, 129.8, 128.7, 128.3, 115.5, 63.3, 55.63, 39.4, 35.6, 31.7, 31.3, 29.2, 22.6, 17.5, 14.1, 13.8.

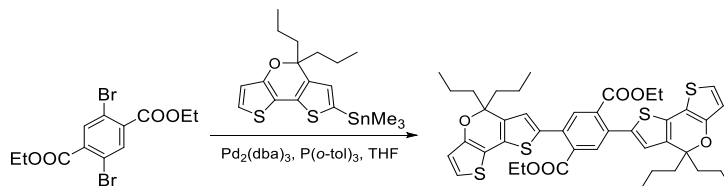
MALDI-TOF MS: Calcd for C<sub>88</sub>H<sub>102</sub>O<sub>2</sub>S<sub>4</sub> (M<sup>+</sup>): 1318.6763, Found: 1318.6766.



**Synthesis of CPDT-4Cl.** A mixture of compound 3 (100 mg, 0.076 mmol, 1.0 eq.) and 2-(5,6-dichloro-3-oxo-2,3-dihydro-1*H*-inden-1-ylidene)malononitrile (100 mg, 0.379 mmol, 5.0 eq.) in chloroform (10 mL) was degassed before pyridine (1 mL) was added. The reaction was kept at 65 °C under N<sub>2</sub> for 1h. The solvent was removed under reduced pressure and the residue was purified by column chromatography (stationary phase: silica gel; eluent: hexane:dichloromethane = 1:2) to get the product as dark blue solid (117 mg, 85%).

<sup>1</sup>H NMR (400 MHz, CDCl<sub>3</sub>) δ 8.85 (s, 2H), 8.72 (s, 2H), 7.84 (s, 2H), 7.42 (s, 2H), 7.31 (d, 8H, *J* = 9.6 Hz), 7.13 (d, 8H, *J* = 8.4 Hz), 2.61 (t, 8H), 1.71-1.55 (m, 12H), 1.52-1.42 (m, 4), 1.42-1.25 (m, 24H), 0.93 (t, 12H), 0.68-0.55 (m, 4H), 0.55-0.29 (m, 16H).  
<sup>13</sup>C NMR (100 MHz, CDCl<sub>3</sub>) δ 186.3, 160.3, 158.4, 153.1, 142.5, 138.9, 138.7, 138.6, 138.2, 136.0, 128.6, 126.7, 124.6, 116.4, 115.1, 114.9, 66.8, 63.4, 55.7, 39.4, 35.6, 31.7, 31.3, 29.2, 22.6, 17.6, 14.1, 13.7.

MALDI-TOF MS: Calcd for C<sub>112</sub>H<sub>106</sub>Cl<sub>4</sub>N<sub>4</sub>O<sub>2</sub>S<sub>4</sub> (M<sup>+</sup>): 1809.5957, Found: 1809.5952.



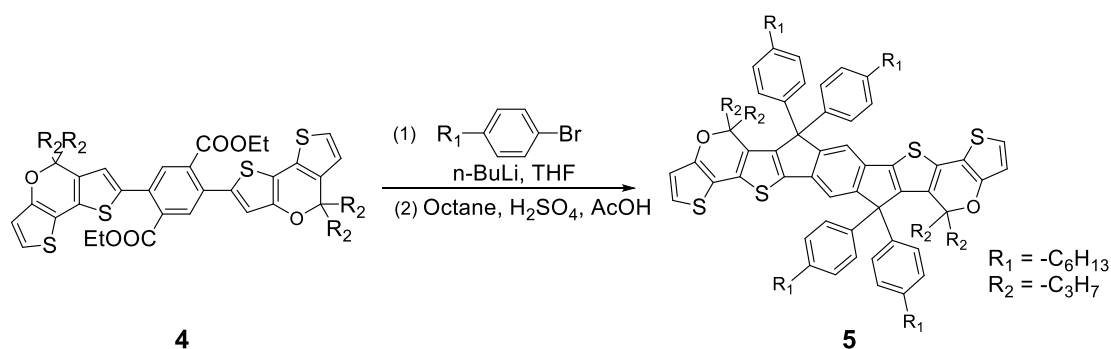
4

**Synthesis of compound 4.** To a mixture of diethyl 2,5-dibromoterephthalate (500 mg, 1.32 mmol), (5,5-dipropyl-5*H*-dithieno[3,2-*b*:2',3'-*d*]pyran-7-yl)trimethylstannane (1.45 g, 3.29 mmol), Pd<sub>2</sub>(dba)<sub>3</sub> (121 mg, 0.132 mmol) and P(*o*-tol)<sub>3</sub> (320 mg, 1.05 mmol) was added anhydrous THF (10 mL) under N<sub>2</sub>. The reaction mixture was stirred for 12 h at 80 °C. Then, the reaction mixture was cooled and poured into an aqueous potassium fluoride. The mixture was extracted with diethyl ether for three times. The combined organic phase was washed with water followed by brine. Then the solution was dried over Na<sub>2</sub>SO<sub>4</sub> and concentrated under reduced pressure. The residue was purified by column chromatography (stationary phase: silica gel; eluent: n-hexane:dichloromethane = 2:1) to get the product as yellow solid (754 mg, 74%).

$^1\text{H}$  NMR (400 MHz,  $\text{CDCl}_3$ )  $\delta$  7.77 (s, 2H), 7.03 (d,  $J = 5.3$  Hz, 2H), 6.73 (s, 2H), 6.70 (d,  $J = 5.3$  Hz, 2H), 4.28 (q, 4H), 1.95-1.80 (m, 8H), 1.57-1.31 (m, 8H), 1.26 (t, 6H), 0.92 (t, 12H).

$^{13}\text{C}$  NMR (100 MHz,  $\text{CDCl}_3$ )  $\delta$  168.1, 151.8, 135.7, 133.7, 133.1, 132.4, 131.2, 130.5, 124.5, 121.4, 118.6, 109.6, 86.3, 61.9, 42.6, 17.2, 14.4, 14.0.

MALDI-TOF MS: Calcd for  $\text{C}_{42}\text{H}_{46}\text{O}_6\text{S}_4$  ( $\text{M}^+$ ): 774.2177, Found: 774.2173.



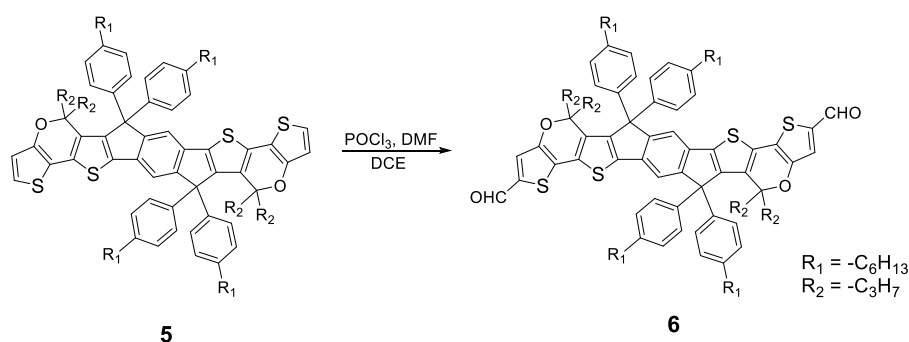
**Synthesis of compound 5.** *n*-BuLi (4.8 mL, 2 M in hexane) was added dropwise to a solution of 1-bromo-4-hexylbenzene (2.34 g, 10.34 mmol) in anhydrous THF (50 mL) at  $-78$  °C under  $\text{N}_2$  atmosphere. The stirred mixture was kept at the same temperature for 1 h and then added into a degassed solution of compound 4 (500 mg, 0.646 mmol) in THF (10 mL) via syringe. When the addition was completed, the resulting mixture was stirred  $-78$  °C for 2 h, followed by quenching with a saturated  $\text{NH}_4\text{Cl}$  solution. The organic layer was separated, and the aqueous phase was extracted with diethyl ether for three times. The combined organic layer was washed with brine, dried over  $\text{MgSO}_4$ , filtered, and concentrated under reduced pressure to obtain a crude diol as a viscous oil, which could be directly used for the next step without further purification.

The crude diol obtained above was dissolved in a mixture of octane (10 mL) and acetic acid (10 mL) and then three drops of concentrated  $\text{H}_2\text{SO}_4$  was added. After being stirred for 1 h at r.t., water was added into the mixture to quench the reaction. The organic layer was separated, and the aqueous phase was extracted with diethyl ether for three times. The combined organic layer was washed with brine, dried over  $\text{MgSO}_4$ , filtered, and

concentrated under reduced pressure. The residue was purified by column chromatography (stationary phase: silica gel; eluent: n-hexane:dichloromethane = 20:1) to get the product as yellow solid (385 mg, 46%).

$^1\text{H}$  NMR (400 MHz,  $\text{CDCl}_3$ )  $\delta$  7.30 (d,  $J = 8.0$  Hz, 8H), 7.09 (d,  $J = 8.0$  Hz, 8H), 7.01 (s, 2H), 6.89 (d,  $J = 4.8$  Hz, 2H), 6.54 (d,  $J = 4.8$  Hz, 2H), 2.59 (t, 8H), 1.61 (t, 8H), 1.43-1.26 (m, 24H), 1.26-1.10 (m, 8H), 1.10-0.95 (m, 8H), 0.88 (t, 12H), 0.36 (t, 12H).  
 $^{13}\text{C}$  NMR (100 MHz,  $\text{CDCl}_3$ )  $\delta$  157.9, 152.1, 141.7, 139.4, 138.3, 133.5, 132.0, 129.0, 128.4, 128.2, 120.4, 117.8, 114.3, 110.4, 88.2, 68.0, 63.9, 43.3, 35.6, 31.8, 31.4, 29.7, 29.1, 25.6, 22.6, 16.69, 14.1, 13.8.

MALDI-TOF MS: Calcd for  $\text{C}_{86}\text{H}_{102}\text{O}_2\text{S}_4$  ( $\text{M}^+$ ): 1294.6763, Found: 1294.6759.



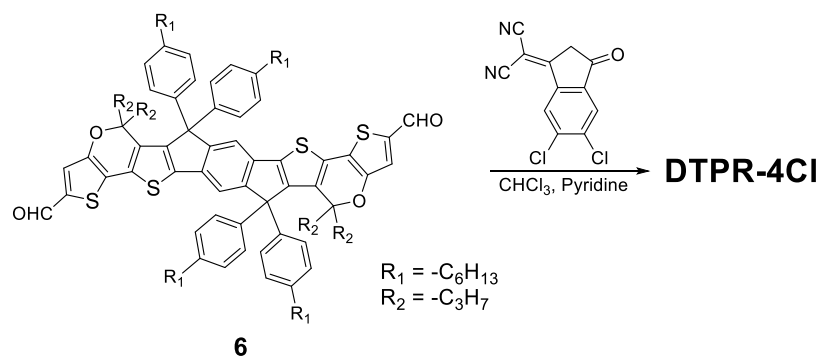
**Synthesis of compound 6.** Compound 5 (200 mg, 0.154 mmol) was dissolved in 20 mL dichloroethane under argon, then the fresh Vilsmeier reagent (0.2 mL  $\text{POCl}_3$  in 1.0 mL DMF) was added dropwise at 0 °C. The mixture was stirred at 85 °C for 3 h. The reaction was quenched with saturated  $\text{Na}_2\text{CO}_3$  solution and allowed to stir at r.t. for 20 mins. The organic layer was separated, and the aqueous phase was extracted with diethyl ether for three times. The combined organic layer was washed with brine, dried over  $\text{MgSO}_4$ , filtered, and concentrated under reduced pressure. The residue was purified by column chromatography (stationary phase: silica gel; eluent: dichloromethane) to get the product as red-purple solid (173 mg, 83%).

$^1\text{H}$  NMR (400 MHz,  $\text{CDCl}_3$ )  $\delta$  9.71 (s, 2H), 7.28 (d,  $J = 8.0$  Hz, 8H), 7.13 (s, 2H), 7.11 (s, 2H), 7.10 (d,  $J = 8.0$  Hz, 8H), 2.59 (t,  $J = 7.7$  Hz, 8H), 1.68-1.55 (m, 8H), 1.38-1.25

(m, 24H), 1.25-1.02 (m, 8H), 1.02-0.84 (m, 8H), 0.91 (t, 12H), 0.36 (t, 12H).

$^{13}\text{C}$  NMR (100 MHz,  $\text{CDCl}_3$ )  $\delta$  181.7, 158.6, 152.4, 152.0, 143.3, 142.1, 137.6, 133.8, 132.7, 128.7, 128.4, 124.4, 122.2, 115.1, 88.7, 64.1, 43.3, 35.5, 31.7, 31.4, 29.1, 22.6, 16.7, 14.1, 13.7.

MALDI-TOF MS: Calcd for  $\text{C}_{88}\text{H}_{102}\text{O}_4\text{S}_4$  ( $\text{M}^+$ ): 1350.6661, Found: 1350.6666.



**Synthesis of compound DTPR-4Cl.** A mixture of compound 6 (100 mg, 0.0740 mmol, 1.0 eq.) and 2-(5,6-dichloro-3-oxo-2,3-dihydro-1*H*-inden-1-ylidene)malononitrile (97 mg, 0.370 mmol, 5.0 eq.) in chloroform (10 mL) was degassed before pyridine (1 mL) was added. The reaction was kept at 65 °C under  $\text{N}_2$  for 1h. The solvent was removed under reduced pressure and the residue was purified by column chromatography (stationary phase: silica gel; eluent: hexane:dichloromethane = 1:2) to get the product as dark blue solid (94 mg, 69%).

$^1\text{H}$  NMR (400 MHz,  $\text{CDCl}_3$ )  $\delta$  8.71 (s, 2H), 8.65 (s, 2H), 7.81 (s, 2H), 7.30 (d,  $J = 8.0$  Hz, 8H), 7.23 (s, 2H), 7.20 (s, 2H), 7.13 (d,  $J = 8.0$  Hz, 8H), 2.60 (t, 8H), 1.62 (m, 8H), 1.45-1.07 (m, 32H), 0.95-0.85 (m, 20H), 0.37 (t, 12H).

$^{13}\text{C}$  NMR (100 MHz,  $\text{CDCl}_3$ )  $\delta$  186.2, 159.5, 157.9, 153.9, 153.4, 148.0, 142.5, 139.1, 138.8, 137.0, 136.6, 136.0, 134.5, 132.4, 131.6, 128.7, 128.6, 126.7, 124.7, 120.1, 115.9, 114.7, 89.2, 68.1, 64.2, 43.4, 35.5, 31.7, 31.4, 29.1, 22.6, 16.7, 14.1, 13.6.

MALDI-TOF MS: Calcd for  $\text{C}_{112}\text{H}_{106}\text{Cl}_4\text{N}_4\text{O}_4\text{S}_4$  ( $\text{M}^+$ ): 1841.5855, Found: 1841.5864.

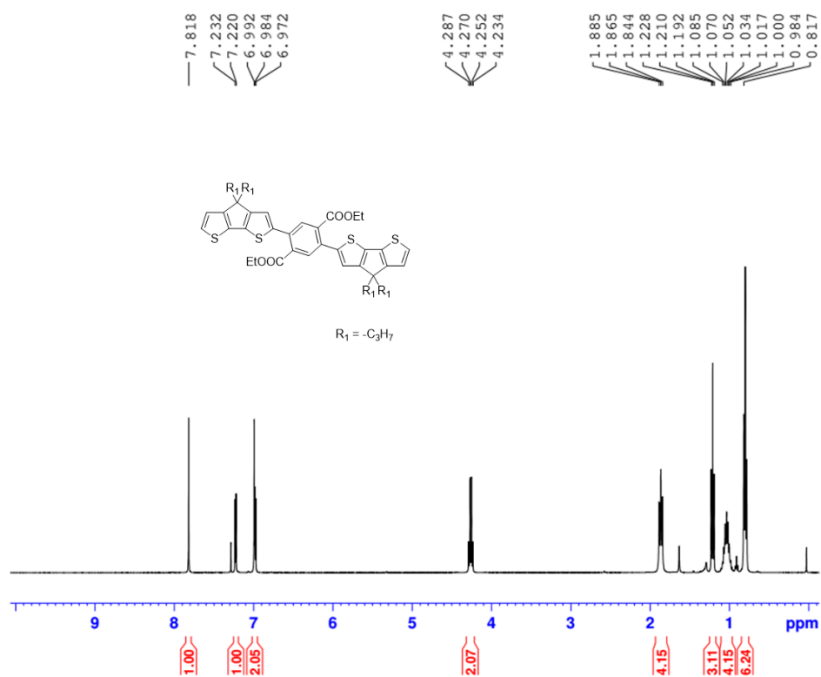


Figure S9.  $^1H$  NMR spectrum of compound 1.

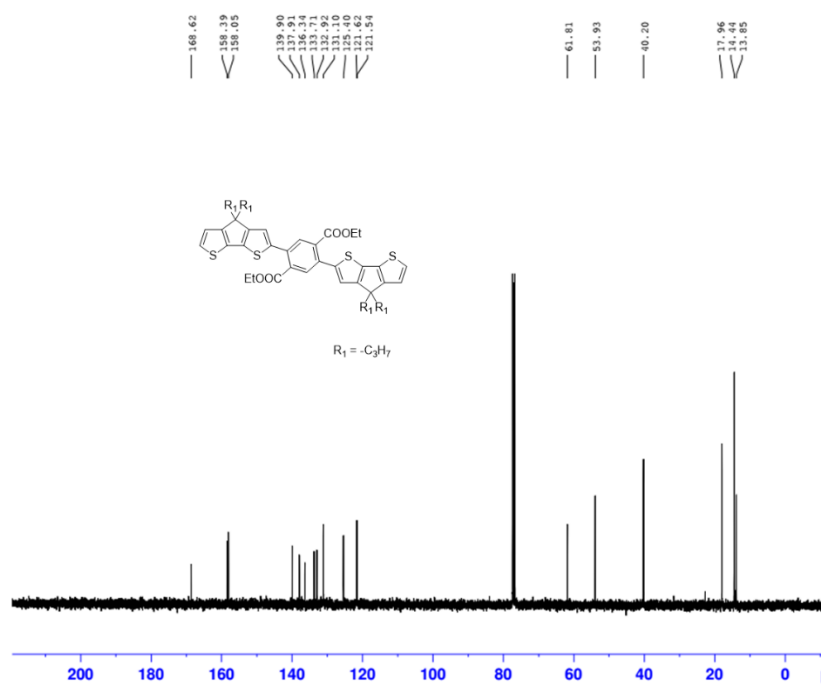


Figure S10.  $^{13}C$  NMR spectrum of compound 1.

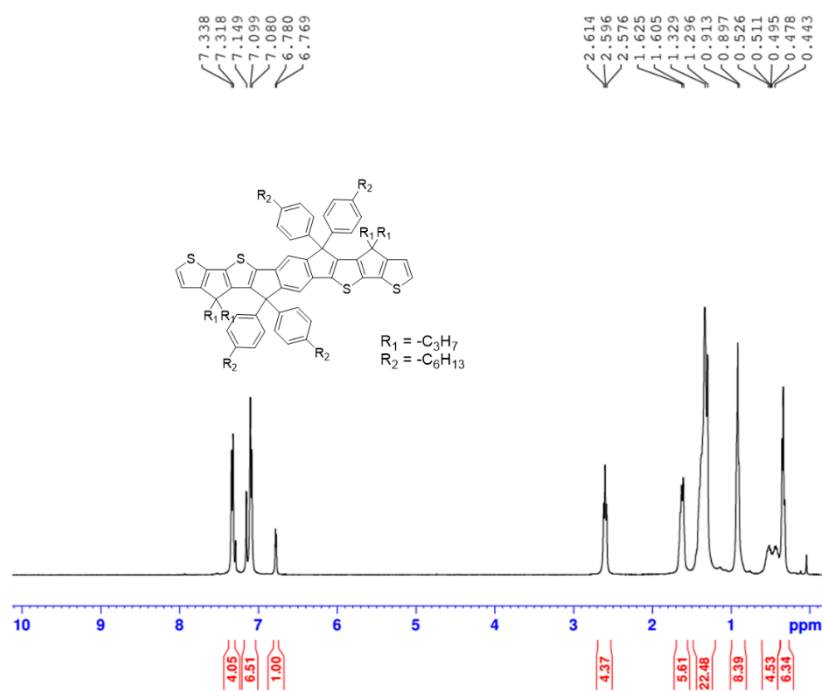


Figure S11.  $^1H$  NMR spectrum of compound 2.

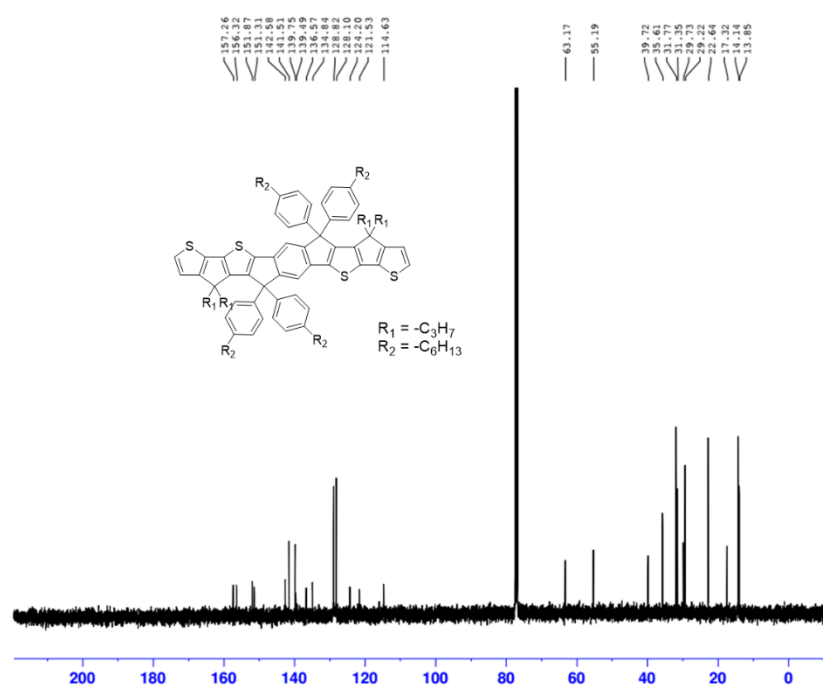


Figure S12.  $^{13}C$  NMR spectrum of compound 2.

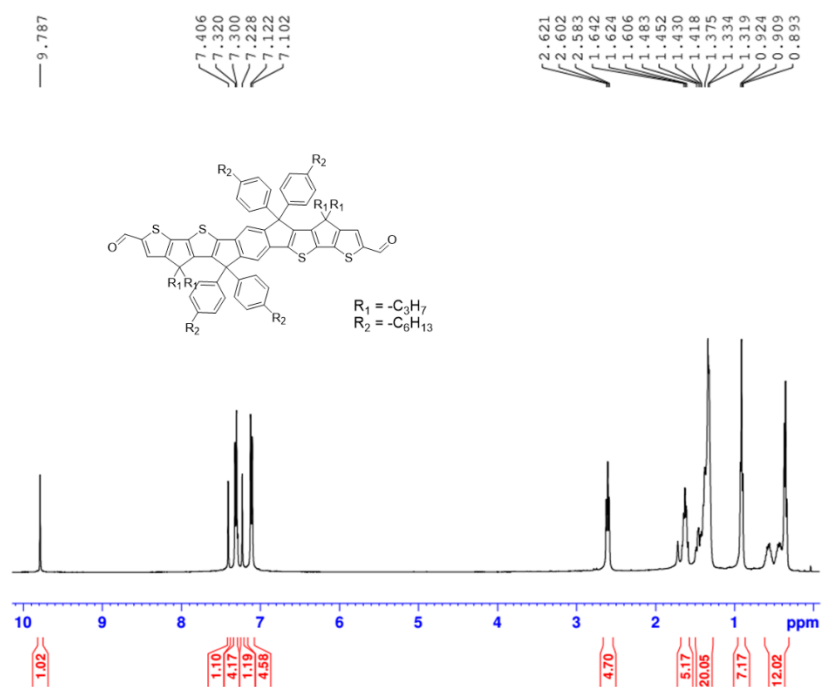


Figure S13.  $^1H$  NMR spectrum of compound 3.

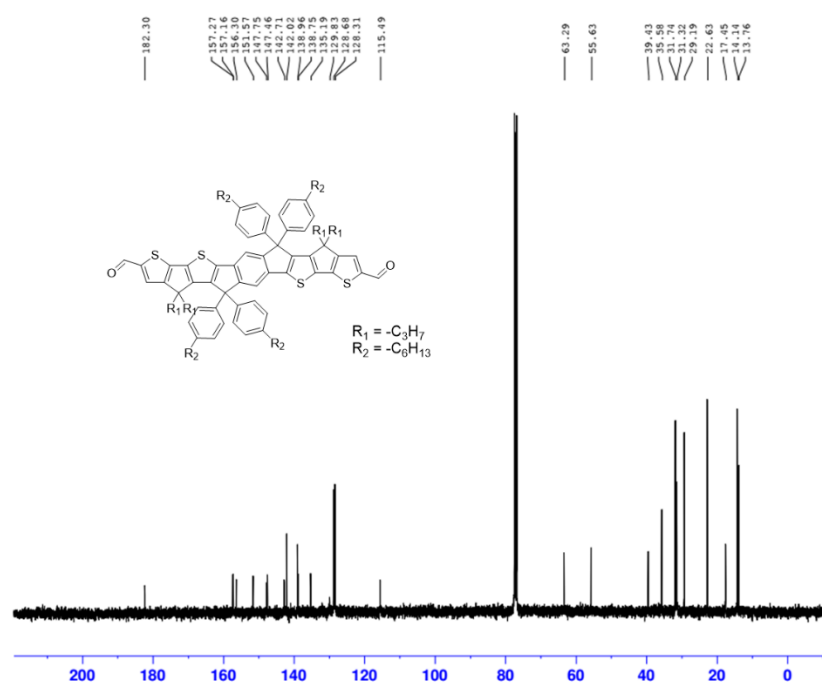


Figure S14.  $^{13}C$  NMR spectrum of compound 3.

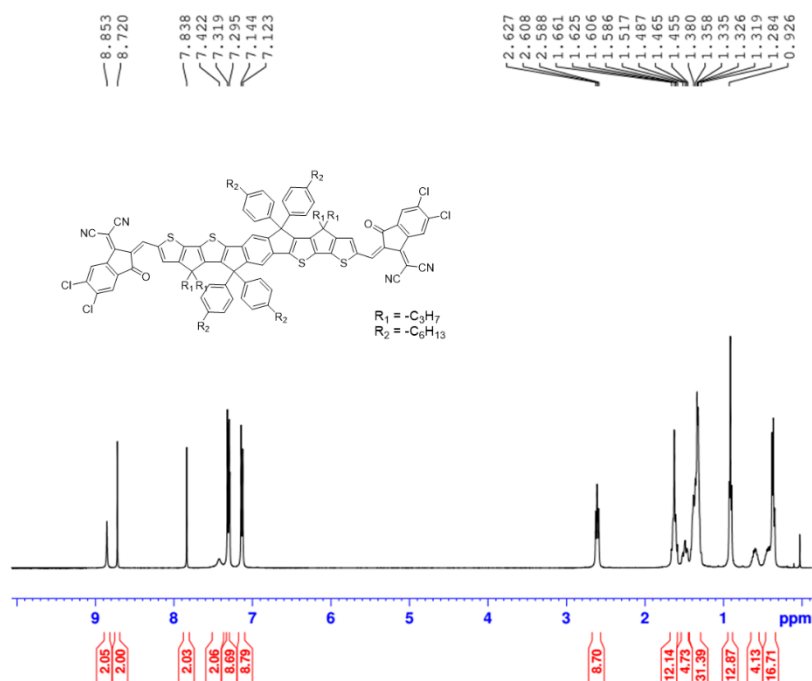


Figure S15.  $^1H$  NMR spectrum of CPDT-4Cl.

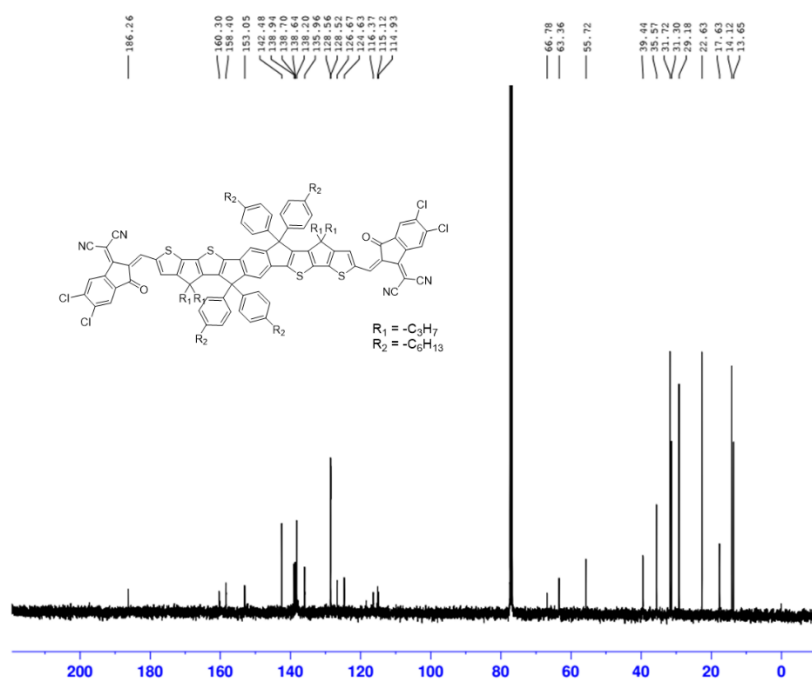


Figure S16.  $^{13}C$  NMR spectrum of CPDT-4Cl.

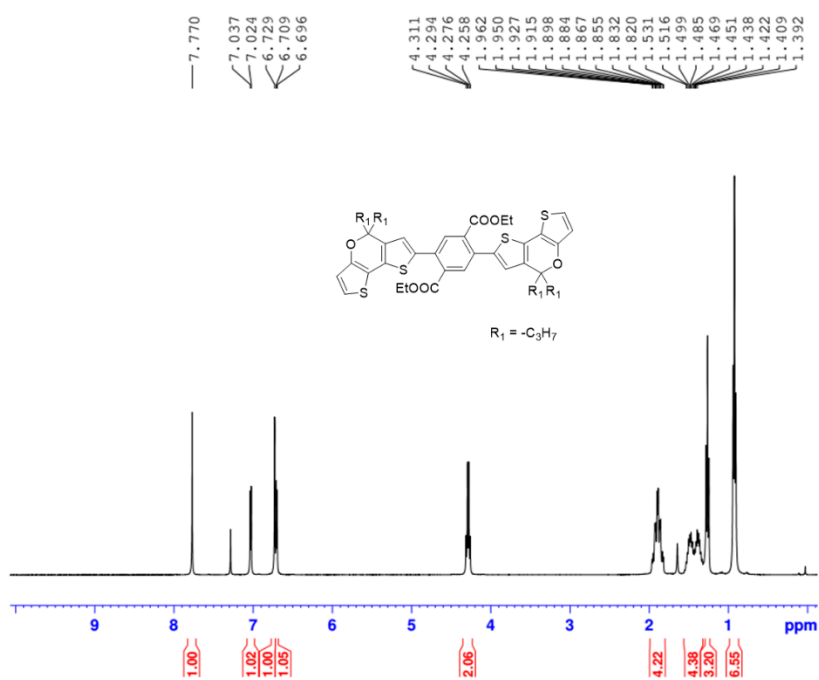


Figure S17. <sup>1</sup>H NMR spectrum of compound 4.

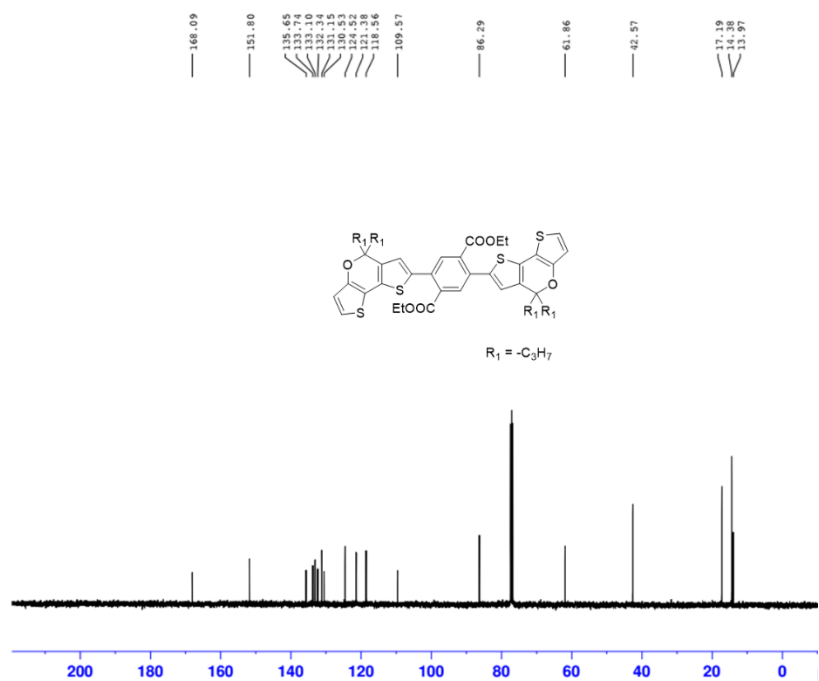


Figure S18. <sup>13</sup>C NMR spectrum of compound 4.

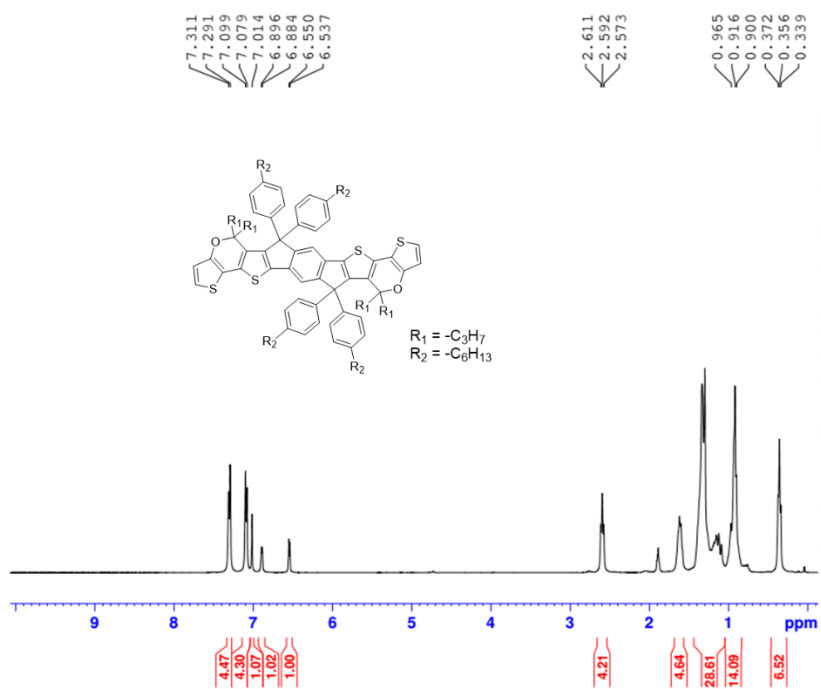


Figure S19.  $^1H$  NMR spectrum of compound 5.

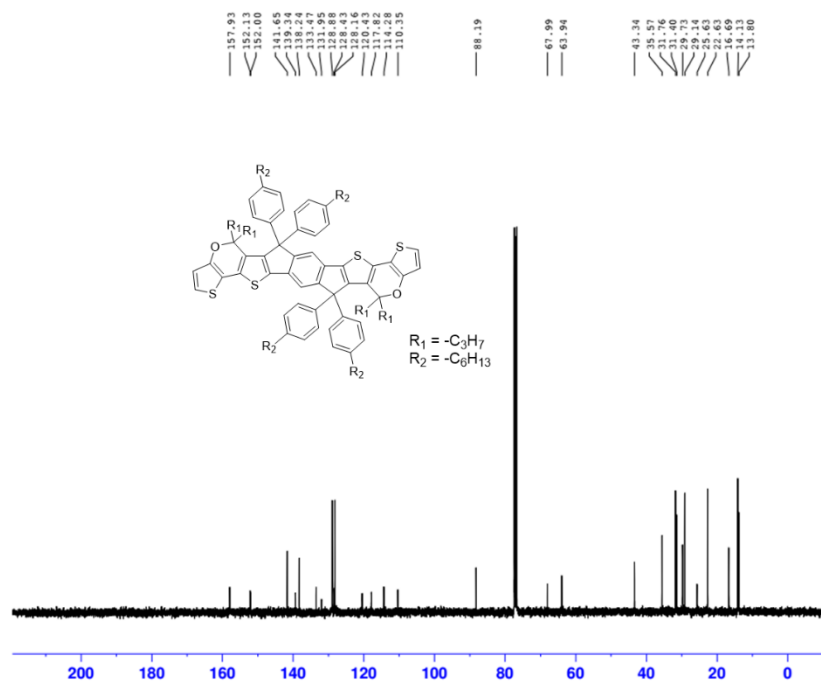


Figure S20.  $^{13}C$  NMR spectrum of compound 5.

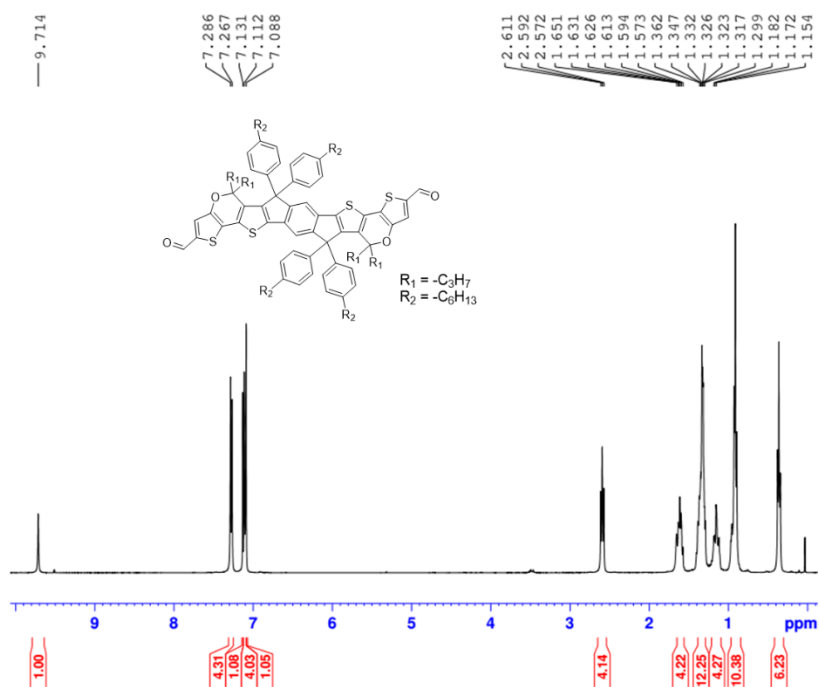


Figure S21. <sup>1</sup>H NMR spectrum of compound 6.

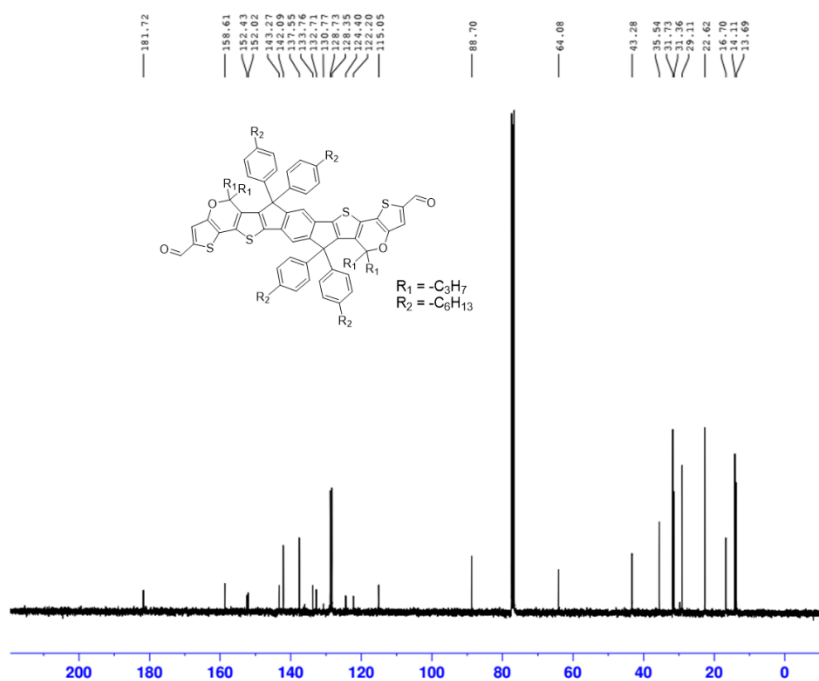


Figure S22. <sup>13</sup>C NMR spectrum of compound 6.

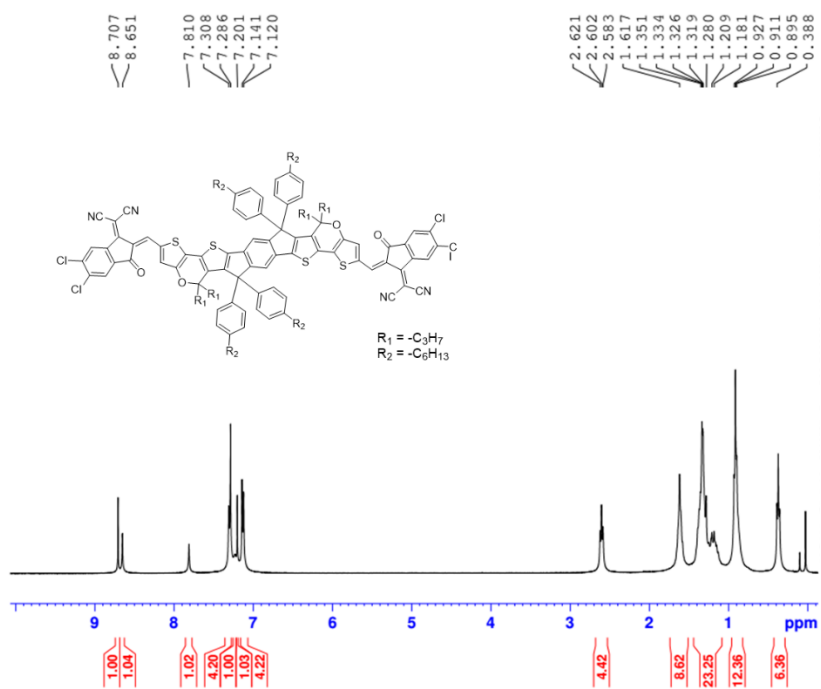


Figure S23.  $^1H$  NMR spectrum of DTPR-4Cl.

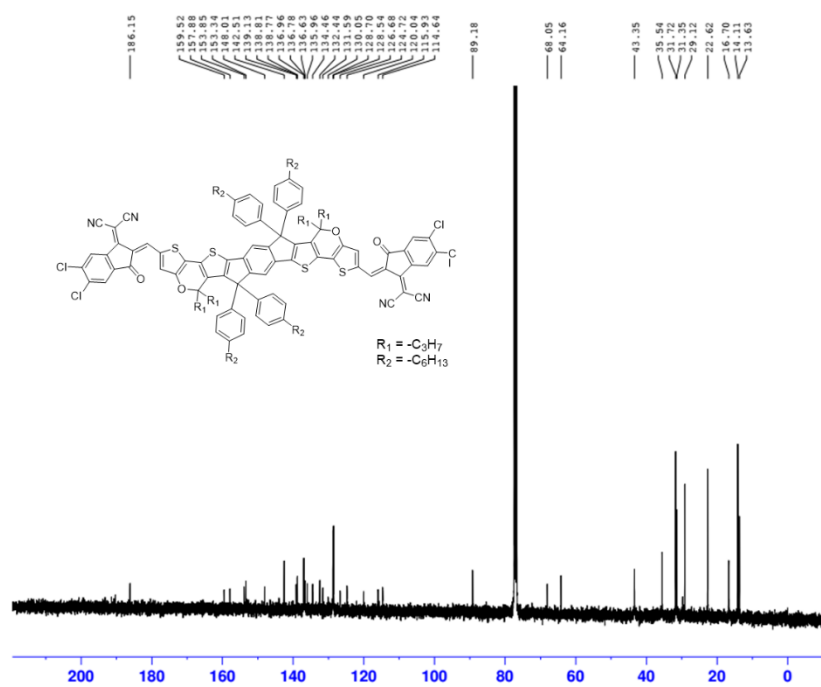


Figure S24.  $^{13}C$  NMR spectrum of DTPR-4Cl.

## Reference

1 D. K. Owens, R. C. Wendt, *J. Appl. Polym. Sci.* **1969**, 13, 1741.